Endocytosis

DOI: 10.1002/anie.201409693

Stiffness-Dependent In Vitro Uptake and Lysosomal Acidification of Colloidal Particles**

*Raimo Hartmann, Marcel Weidenbach, Martin Neubauer, Andreas Fery, and Wolfgang J. Parak**

Abstract: *The physico-chemical properties of colloidal particles determine their uptake into cells. For a series of microparticles only one parameter, the mechanical stiffness, was varied, whereas other parameters such as size, shape, and charge were kept constant. The uptake was monitored in situ by analyzing individual particle trajectories including the progress of endocytosis, derived from local pH measurements around each particle. Evidence is presented that soft particles with low stiffness are transported faster to lysosomes than stiffer ones.*

The number of applications based on the interaction of colloids with cells has been increasing steadily over the past few years, mostly for sensing- or delivery-based applications. As most of the approaches require particle internalization, cellular uptake mechanisms have been heavily studied.[1] Unfortunately, the ultimate goal, to entirely correlate the uptake process with the physico-chemical particle properties, is not trivial, in particular as many of these properties are interrelated.[2] Thus, it is extremely challenging to obtain consistent studies, in which only one particular parameter of the particles is varied, while all other properties are held constant. Properties that have been studied systematically comprise particle size,[3] shape,[4] and charge.[5] While size, shape, and charge are the "standard" well-investigated parameters influencing in vitro particle incorporation by cells, there are many additional well-defined physical properties, for instance particle stiffness, which might also play an important role. Dependent on their stiffness, hollow microparticles are compressed and deformed upon cellular internalization.[6,7] Based on theoretical considerations Yi et al. claimed that cellular processing of deformable particles might be different to that of stiffer counterparts, because these particles are less prone to membrane wrapping.[8] Hydrogel-based nanoparticles with a Young's modulus between 30 and 140 kPa were found to be internalized more efficiently by RAW 264.7 macrophages than softer (< 30 kPa) or stiffer (> 140 kPa) nanoparticles.[9] Liu et al. reported that the uptake rate of flexible micron-sized hydrogel particles (15–35 kPa) was higher than that of less elastic ones (75–160 kPa) by HepG2 cells.[10]

Polymer capsules, for example, hollow microparticles synthesized by layer-by-layer (LbL) assembly of oppositely charged polyelectrolytes,[11] are a well-suited model system for systematic investigations, since their various physico-chemical properties can be tuned independently.[12] Size[13] and shape[14] can be varied by using different template cores, and the sign of the surface charge is simply determined by the charge of the outermost layer. Stiffness can be tuned by variation of the number of polymer layers or by the polymer materials used.[15,16] Thus, polyelectrolyte capsules are a convenient particle system to investigate stiffness-dependent in vitro uptake by cells, in a way such that particle size, shape, charge, and surface chemistry remain constant, while stiffness is varied. Most important, with this system it is possible to change exclusively one parameter, whereby the outer surface remains the same, and physicochemical parameters other than stiffness are fully maintained.

Upon internalization, capsules (i.e. particles) are taken up via endocytic processes and are transferred from the neutral extracellular medium to increasingly acidic intracellular vesicles of different maturity, and finally end up in the lysosome.[17] The local pH around each particle can be used as readout that describes its present stage of uptake. For this purpose particles can be loaded with pH-sensitive fluorophores such as fluorescein-based dyes[18,19] and seminaphtharhodafluor (SNARF),[19,20] which allow for the time-resolved detection of the local pH around the capsules in extra- and intracellular environments.[6,20,21]

Based on LbL assembly[11] around sacrificial $CaCO_3$ template cores we synthesized pH-sensitive capsules with a different number of layers to vary capsule stiffness with two frequently used polymer systems (nondegradable polymers: poly(sodium 4-styrenesulfonate) (PSS) and poly(allylamine hydrochloride) (PAH); degradable polymers: dextran sulfate sodium salt (DextS) and poly-L-arginine hydrochloride (PLArg);[17,22] cf. Figure 1a). Two batches of template cores with resulting diameters of 4.1 μm (size "S") and 4.7 μm (size "L") were used. The pH sensitivity was achieved by embedding SNARF-1[19,20]-labeled dextran into the cavity of the capsules. Response curves relating the ratio of red (I_r; 615–700 nm) to yellow (I_g; 560–615 nm, shown in green) fluorescence I_r/I_g(pH) were obtained for each type of capsule (Figure 1b). With this setup changes in pH could be monitored down to values around 4.5. However, SNARF-1

[*] R. Hartmann, M. Weidenbach, Prof. W. J. Parak
Fachbereich Physik, Philipps Universität Marburg
35037 Marburg (Germany)
E-mail: wolfgang.parak@physik.uni-marburg.de
Prof. W. J. Parak
CIC BiomaGUNE, 20009 San Sebastian (Spain)
M. Neubauer, Prof. A. Fery
Fakultät für Chemie, Universität Bayreuth (Germany)

[**] This work was supported by LOEWE (project Synchembio to W.J.P.). We thank Dr. Andreas Schaper for his kind introduction into ultrasectioning and Dr. Pilar Rivera Gil for stimulating technical discussions at the initial stages of this work.

Supporting information for this article is available on the WWW under http://dx.doi.org/10.1002/anie.201409693.

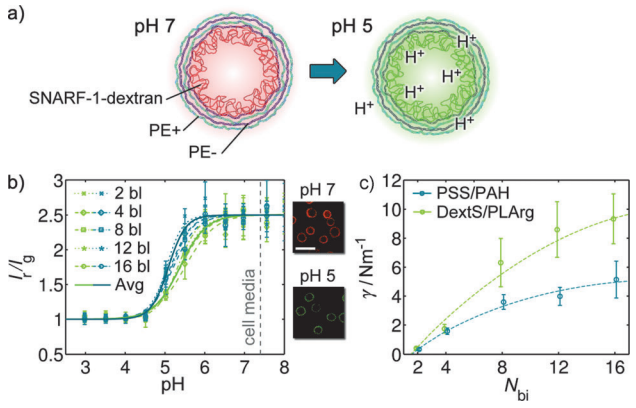

Figure 1. a) Sketch of one polyelectrolyte capsule, which comprises $N_{bi}=2$ bilayers, each composed out of one negatively charged (PE− (purple), PSS, or DextS) and one positively charged (PE+ (light blue), PAH, or PLArg) polyelectrolyte layer. Due to the positively charged outermost layer the whole particle is positively charged (cf. Figure SI-7). pH-sensitive fluorophores SNARF-1 conjugated to dextran are located inside the cavity. b) The red-to-green ratio (false colors) of the fluorescence signal I_r/I_g from the capsule cavity depends on the local pH around each capsule. Response curves are shown for capsules of 2–16 bilayers (bl) of size "S" (green: DextS/PLArg, blue: PSS/PAH) and are normalized to pH 7.4 (cell media). The solid lines (labeled "Avg") show the average response curves for both types. The insets (scale bar: 2 μm) show fluorescence microscopy images of capsules at neutral (red fluorescence) and acidic pH (green fluorescence). c) The dependence of the mechanical stiffness γ for the different capsules ($d\approx4.1$ μm, size "S") as determined by AFM is plotted versus on the number of bilayers N_{bi} making up the capsule shell. The dashed lines are guides to the eye only.

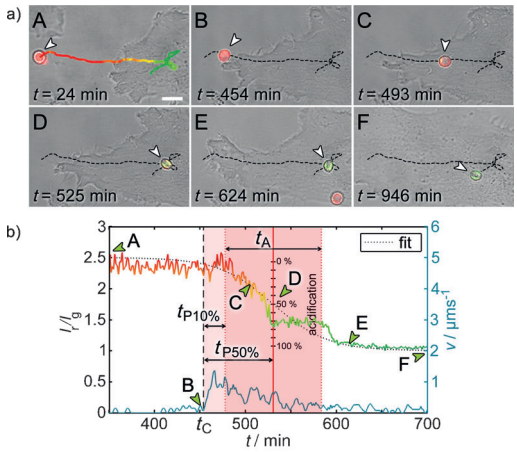

Figure 2. a) Typical timelapse recording of one PSS/PAH capsule ($N_{bi}=8$, size "L") during its uptake by a HeLa cell. The images (overlay of green and red fluorescence and the brightfield micrograph) recorded at a temporal resolution of 120 s are used to determine the trajectory of the capsule (scale bar: 5 μm). b) The ratio of red-to-green fluorescence I_r/I_g of the capsule has been determined for each image and is plotted versus the incubation time t. The time points corresponding to the images in (a) are labeled A–F. A ratio of $I_r/I_g\approx2.5$ corresponds to a pH 7.4, while $I_r/I_g\approx1$ corresponds to local pH < 4.5 (Figure 1b). The acidification time t_A reflects the duration of the acidification process while the processing time $t_{P10\%}$ is determined as the period from the first contact of the capsule with the cell (B, high velocity) until the beginning of the acidification process (red area) and $t_{P50\%}$ as the period until the point of inflection of the readout curve (D).

embedded in biodegradable DextS/PLArg capsules was slightly less sensitive at lower pH values.

The stiffness of the capsules in solution was determined by atomic force microscopy (AFM) for each type of capsule[16] (Figure 1c). As expected, the stiffness of the capsules increased with the number of polyelectrolyte layers. Presumably this is a direct consequence of the shell thickness, which increases with the number of polyelectrolyte layers. In particular, in case of the DextS/PLArg capsules there were batch-to-batch variations of the absolute stiffness values (cf. the Supporting Information (SI), Figure SI-5).

The uptake process was monitored in different adherent cells (cell lines as well as primary cells). Upon internalization, the local environment of the capsules changed from neutral (cell medium) to strongly acidic (lysosome), which can be seen by the ratiometric readout of the pH-sensitive fluorophores embedded in the capsules[20,21] (Figure 2a). First (image A), each capsule is located in neutral/slightly alkaline cell medium, thus leading to high, constant I_r/I_g values. At one point in time, here defined as t_C, the particle touches the cell surface (image B) and then it moves along the outer plasma membrane, as visible by the red emission which demonstrates extracellular location. It is then engulfed by the cell, as visualized by the change in fluorescence, and subsequently passed to more and more acidic compartments (images C and D), until at one point the pH seems to remain constant. At this point (image E) the capsule reaches its final destination, the lysosome.[17] If the pH decreases below 4.5 changes to an even more acidic environment are no longer observable due to the limited sensitivity of the pH indicator used (Figure 1b). Figure 2b shows that the pathway of uptake is not necessarily continuous, as can be seen by the jump of the pH values along the trace in image D at $t=525$ min. We speculate that at this point in time the capsule-containing vesicular compartment may have fused with a vesicle of potentially much lower pH. (A correlation of fusion events of acidic vesicles with the pH values of the capsule-containing compartment can be found in Figure SI-16.) In order to derive quantitative data from the $I_r/I_g(t)$ traces we define t_A as the acidification time and $t_{P10\%}/t_{P50\%}$ as the processing time. The processing time is the duration from the first contact t_C (membrane attachment) of the capsule with the cell, following its incorporation and finally partial acidification (10% or 50%). The acidification time describes the duration of acidification from high to low pH following the sigmoidally shaped time-dependent $(I_r/I_g)(t)$ curve (Figure 2b, for more details see Figure SI-9).

The uptake of microcapsules can differ significantly between different cell types and capsule materials.[6,17] In most previous studies research focused on quantifying the amount of incorporated capsules versus time, while in this work the acidification and processing time of individual capsules was quantified during uptake. Whereas PSS/PAH and DextS/PLArg capsules are differently processed by cells (nondegradable versus degradable),[22] both are internalized in a similar way and are ultimately located in the lysosomes.[17] It has to be noted that the acidification time and processing time, t_A and $t_{P50\%}$, respectively, depend on the cell line used

(see Figure SI-14). There is also a significant difference between the capsule types (PSS/PAH versus DextS/PLArg, and batch "S" versus "L") regarding $t_{A,}$ while the values for $t_{P50\%}$ are comparable for both materials. The differences are more distinct for HeLa cells than for phagocytes such as monocyte-derived macrophages (MDM) and monocyte-derived dendritic cells (MDDC), which are known for rapid phagocytosis of micron-sized particles.

In the following we focused on HeLa cells, in order to probe for the dependence of uptake on the stiffness of the capsules (as calibrated in Figure 1c). The data shown in Figure 3a demonstrate that independent of the particle size of the nondegradable PSS/PAH capsules the acidification time t_A

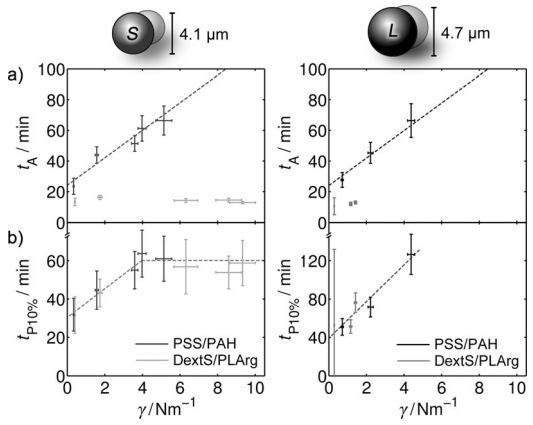

Figure 3. a) Acidification time t_A and b) processing time $t_{P10\%}$ of PSS/PAH and DextS/PLArg capsules with variable number of bilayers N_{bi} and different average diameters as recorded upon incubation with HeLa cells. For each number of bilayers N_{bi} the stiffness γ was taken from Figure 1c and then t_A and $t_{P10\%}$ were plotted against γ. Each data point corresponds to the median t_A or $t_{P10\%}$ value including confidence intervals (y axis) versus the mean stiffness γ value $\pm$ standard error (x axis), as obtained from at least 80 capsules (time values) and 40 capsules (stiffness values). The dashed lines are guides to the eye only. Please note that the large error bars in (b) for $t_{P10\%}$ and DextS/PLArg capsules ($N_{bi}=1$, size "L") result from the fact that these capsules are extremely fragile and thus the determination of t_C (membrane attachment) is challenging.

increases linearly with capsule stiffness γ, whereas for degradable DextS/PLArg capsules there is no such dependency. In other words, for the degradable capsules the transition from neutral/slightly alkaline extracellular pH to the highly acidic pH of lysosomes is faster. In comparison, for the nondegradable capsules the duration of this process is longer and in addition becomes even slower with increasing capsule stiffness. The dwelling time for the capsules in the cascade of intracellular vesicles during internalization thus may be different for the two types of capsules. In contrast, the processing time $t_{P10\%}$ increases with the stiffness for both capsules, for $\gamma < 5\ \mathrm{N\,m^{-1}}$ in a first approximation even linearly (Figure 3b). Hence, $t_{P10\%}$ is universally determined by γ. The acidification time only reflects the duration of the event where the local pH of the particle-containing vesicle is lowered, whereas the processing time also comprises the full uptake process. This involves the duration of engulfment by the cellular plasma membrane, pinching-off into an endocytic vesicle, and subsequent processing to more acidic environments. While t_A is fully derived from a sigmoidal fit to the response function $I_r/I_g(t)$, it is not biased. In contrast, the processing time requires the determination of the time of first contact t_C with the cellular plasma membrane for each capsule. Hence, this parameter is less robust, as t_C is difficult to determine accurately especially if the substrate is very crowded and particles are passed between cells before they are fully endocytosed. From our results we conclude that the uptake itself and the subsequent endosomal trafficking is strongly dependent on the stiffness of the particle, while further processing and acidification is governed mainly by the particle chemistry.

After contact with cells up to their internalization, particles undergo a cascade in which the particle-containing intracellular vesicles grow steadily in size, for example by fusion with other (smaller) vesicles.[23] From a mechanistic point of view one can regard this cascade as an intracellular sorting mechanism. Particles are passed from one vesicle to a subsequently larger one by fusion. Upon each fusion step the pH is lowered, which has been observed by fluorescence staining of acidic vesicles while the pH value around the capsule is recorded (see Figure SI-16). In a simplified view one can imagine that upon such sorting the stiffness plays a decisive role. The more flexible the particle, the better it can adopt its shape and allow evolution of vesicular containers. Thus, less deformable, that is, stiffer particles that can follow shape fluctuations to a lesser degree are more prone to delay their processing within this cascade. The same has been observed for particles that are agglomerated and therefore less "flexible" towards well-dispersed particles.[23] Our data clearly demonstrate that the transport of particles from the outer cellular membrane to the lysosome is determined by the mechanical properties of the particles, that is, by the stiffness of the particles.

One might speculate that these findings could be reciprocal. This would lead to a situation in which cells with higher deformability would be more efficient at incorporating a given type of particle. For such an analysis the data shown in Figure 3b would need to be related with the stiffness of cells. It is clearly known from the literature that cell stiffness can differ significantly for different cells types. For instance, cancerous cells are softer than their noncancerous counterparts (MCF7 versus MCF10).[24] While measurements of cell stiffness as obtained with optical tweezers indicate the global stiffness of cells in suspension,[24] measurements with AFM indicate the local stiffness of adherent cells.[25,26] The softest part of a cell is the nuclear region and the cell becomes stiffer towards its exterior regions.[26] Concerning the cells as investigated in this study, the following elastic moduli are known from the literature: HeLa: (105 ± 17) kPa[27] and (13 ± 7) kPa,[28] A549: (12 ± 5) kPa,[29] MDM: (44 ± 9) kPa (podosome-containing regions) versus (8 ± 2) kPa (podosome-free regions)[30] and HUVEC: (6 ± 5) kPa.[26] If we compare these values with our data shown in Figure SI-15 no direct correlation of processing times t_P with the elastic moduli E of cells can be concluded, which is likely because these values cannot be compared directly to those from other studies. For

such data future AFM experiments would be required, in which the elastic moduli are recorded under controlled conditions.

Our study demonstrates how the cellular uptake of particles indeed is controlled by basic physico-chemical parameters such as low stiffness. A comprehensive picture about such dependencies will make it possible to synthesize particles with defined cellular interaction patterns. In addition the introduced system might improve our understanding of specific endocytic mechanisms related to lysosomal acidification.

Experimental Section

Polyelectrolyte capsules composed out of different polymers (biodegradable/non-biodegradable) and having different stiffnesses (adjusted by varying the number of adsorbed layers) loaded with SNARF-1 were synthesized according to procedures described in the literature.[17,21,22] Force spectroscopy measurements in aqueous solution were performed with a Nanowizard I device from JPK Instruments. The capsule uptake by cells (HeLa, A549, MDM, MDDC, SH-SY5Y, and HUVEC) was monitored by confocal laser scanning microscopy (LSM Meta 510, Zeiss) with a temporal resolution of $\Delta t <$ 2 min. Image processing and capsule tracking was performed with Matlab (MathWorks). A detailed description can be found in the Supporting Information.

Received: October 2, 2014
Published online: December 5, 2014

Keywords: biosensors · mechanical properties · nanoparticles · polymeric capsules

[1] S. Parveen, R. Misra, S. K. Sahoo, *Nanomed. Nanotechnol.* **2012**, *8*, 147.
[2] P. Rivera-Gil, D. Jimenez de Aberasturi, V. Wulf, B. Pelaz, P. del Pino, Y. Zhao, J. de La Fuente, I. Ruiz de Larramendi, T. Rojo, X.-J. Liang, et al., *Acc. Chem. Res.* **2013**, *46*, 743.
[3] a) W. Jiang, B. Y. S. Kim, J. T. Rutka, W. C. W. Chan, *Nat. Nanotechnol.* **2008**, *3*, 145; b) S. L. Zhang, J. Li, G. Lykotrafitis, G. Bao, S. Suresh, *Adv. Mater.* **2009**, *21*, 419.
[4] L. C. Stoehr, E. Gonzalez, A. Stampfl, E. Casals, A. Duschl, V. Puntes, G. J. Oostingh, *Part. Fibre Toxicol.* **2011**, *8*, 3.
[5] a) A. Muñoz Javier, O. Kreft, A. Piera Alberola, C. Kirchner, B. Zebli, A. S. Susha, E. Horn, S. Kempter, A. G. Skirtach, A. L. Rogach, et al., *Small* **2006**, *2*, 394; b) D. Hühn, K. Kantner, C. Geidel, S. Brandholt, I. De Cock, S. J. H. Soenen, P. Rivera Gil, J.-M. Montenegro, K. Braeckmans, K. Müllen, et al., *ACS Nano* **2013**, *7*, 3253.
[6] A. Muñoz Javier, O. Kreft, M. Semmling, S. Kempter, A. G. Skirtach, O. Bruns, P. d. Pino, M. F. Bedard, J. Rädler, J. Käs, et al., *Adv. Mater.* **2008**, *20*, 4281.
[7] R. Palankar, B.-E. Pinchasik, S. Schmidt, B. G. De Geest, A. Fery, H. Möhwald, A. Skirtach, M. Delcea, *J. Mater. Chem. B* **2013**, *1*, 1175.
[8] X. Yi, X. H. Shi, H. J. Gao, *Phys. Rev. Lett.* **2011**, *107*, 098101.
[9] X. Banquy, F. Suarez, A. Argaw, J. M. Rabanel, P. Grutter, J. F. Bouchard, P. Hildgen, S. Giasson, *Soft Matter* **2009**, *5*, 3984.
[10] W. Liu, X. Zhou, Z. Mao, D. Yu, B. Wang, C. Gao, *Soft Matter* **2012**, *8*, 9235.
[11] J. Borges, J. F. Mano, *Chem. Rev.* **2014**, *114*, 8883.
[12] E. Donath, G. B. Sukhorukov, F. Caruso, S. A. Davis, H. Möhwald, *Angew. Chem. Int. Ed.* **1998**, *37*, 2201; *Angew. Chem.* **1998**, *110*, 2323.
[13] a) H. G. Zhu, E. W. Stein, Z. H. Lu, Y. M. Lvov, M. J. McShane, *Chem. Mater.* **2005**, *17*, 2323; b) C. S. Peyratout, L. Dähne, *Angew. Chem. Int. Ed.* **2004**, *43*, 3762; *Angew. Chem.* **2004**, *116*, 3850.
[14] a) O. Shchepelina, V. Kozlovskaya, E. Kharlampieva, W. Mao, A. Alexeev, V. V. Tsukruk, *Macromol. Rapid Commun.* **2010**, *31*, 2041; b) A. Yashchenok, B. Parakhonskiy, S. Donatan, D. Kohler, A. Skirtach, H. Mohwald, *J. Mater. Chem. B* **2013**, *1*, 1223; c) O. Shimoni, Y. Yan, Y. Wang, F. Caruso, *ACS Nano* **2013**, *7*, 522.
[15] C. Gao, E. Donath, S. Moya, V. Dudnik, H. Mohwald, *Eur. Phys. J. E* **2001**, *5*, 21.
[16] a) F. Dubreuil, N. Elsner, A. Fery, *Eur. Phys. J. E* **2003**, *12*, 215; b) A. Fery, R. Weinkamer, *Polymer* **2007**, *48*, 7221.
[17] L. Kastl, D. Sasse, V. Wulf, R. Hartmann, J. Mircheski, C. Ranke, S. Carregal-Romero, J. A. Martínez-López, R. Fernández-Chacón, W. J. Parak, et al., *ACS Nano* **2013**, *7*, 6605.
[18] U. Reibetanz, M. H. A. Chen, S. Mutukumaraswamy, Z. Y. Liaw, B. H. L. Oh, S. Venkatraman, E. Donath, B. Neu, *Biomacromolecules* **2010**, *11*, 1779.
[19] L. L. del Mercato, A. Z. Abbasi, W. J. Parak, *Small* **2011**, *7*, 351.
[20] O. Kreft, A. Muñoz Javier, G. B. Sukhorukov, W. J. Parak, *J. Mater. Chem.* **2007**, *17*, 4471.
[21] P. Rivera-Gil, M. Nazarenus, S. Ashraf, W. J. Parak, *Small* **2012**, *8*, 943.
[22] P. Rivera-Gil, S. D. Koker, B. G. De Geest, W. J. Parak, *Nano Lett.* **2009**, *9*, 4398.
[23] C. Brandenberger, C. Mühlfeld, Z. Ali, A.-G. Lenz, O. Schmid, W. J. Parak, P. Gehr, B. Rothen-Rutishauser, *Small* **2010**, *6*, 1669.
[24] B. Lincoln, H. M. Erickson, S. Schinkinger, F. Wottawah, D. Mitchell, S. Ulvick, C. Bilby, J. Guck, *Cytometry Part A* **2004**, *59A*, 203.
[25] J. Domke, S. Dannöhl, W. J. Parak, O. Müller, W. K. Aicher, M. Radmacher, *Colloids Surf. B* **2000**, *19*, 367.
[26] T. G. Kuznetsova, M. N. Starodubtseva, N. I. Yegorenkov, S. A. Chizhik, R. I. Zhdanov, *Micron* **2007**, *38*, 824.
[27] A. Berquand, A. Holloschi, M. Trendelenburg, P. Kioschis, *Microsc. Today* **2010**, *19*, 34.
[28] J. Ren, S. Yu, N. Gao, Q. Zou, *Phys. Rev. E* **2013**, *88*, 052711.
[29] L. Xiao, M. Tang, Q. Li, A. Zhou, *Anal. Methods* **2013**, *5*, 874.
[30] A. Labernadie, C. Thibault, C. Vieu, I. Maridonneau-Parini, G. M. Charrière, *Proc. Natl. Acad. Sci. USA* **2010**, *107*, 21016.

